Neuropsychologia 51 (2013) 2352–2359

Contents lists available at ScienceDirect

Neuropsychologia

journal homepage: www.elsevier.com/locate/neuropsychologia

Differential roles for medial prefrontal and medial temporal cortices in schema-dependent encoding: From congruent to incongruent

Marlieke T.R. van Kesteren [a,b,*,1], Sarah F. Beul [a,c,1], Atsuko Takashima [d], Richard N. Henson [e], Dirk J. Ruiter [b], Guillén Fernández [a,f]

[a] Radboud University Nijmegen, Donders Institute for Brain, Cognition and Behaviour, P.O. Box 9101, 6500 HB Nijmegen, The Netherlands
[b] Radboud University Nijmegen Medical Centre, Department of Anatomy, P.O. Box 9101, 6500 HB Nijmegen, The Netherlands
[c] Department of Computational Neuroscience, University Medical Center Hamburg-Eppendorf, Martinistraße 52, 20246 Hamburg, Germany
[d] Radboud University Nijmegen, Behavioural Science Institute, P.O. Box 9101, 6500 HB Nijmegen, The Netherlands
[e] MRC Cognition & Brain Sciences Unit, Cambridge CB2 7EF, UK
[f] Radboud University Nijmegen Medical Centre, Department of Neuroscience, P.O. Box 9101, 6500 HB Nijmegen, The Netherlands

ARTICLE INFO

Available online 13 June 2013

Keywords:
Schema
Congruency
Memory encoding
Medial temporal lobe
Medial prefrontal cortex

ABSTRACT

Information that is congruent with prior knowledge is generally remembered better than incongruent information. This effect of congruency on memory has been attributed to a facilitatory influence of activated schemas on memory encoding and consolidation processes, and hypothesised to reflect a shift between processing in medial temporal lobes (MTL) towards processing in medial prefrontal cortex (mPFC). To investigate this shift, we used functional magnetic resonance imaging (fMRI) to compare brain activity during paired-associate encoding across three levels of subjective congruency of the association with prior knowledge. Participants indicated how congruent they found an object-scene pair during scanning, and were tested on item and associative recognition memory for these associations one day later. Behaviourally, we found a monotonic increase in memory performance with increasing congruency for both item and associative memory. Moreover, as hypothesised, encoding-related activity in mPFC increased linearly with increasing congruency, whereas MTL showed the opposite pattern of increasing encoding-related activity with decreasing congruency. Additionally, mPFC showed increased functional connectivity with a region in the ventral visual stream, presumably related to the binding of visual representations. These results support predictions made by a recent neuroscientific framework concerning the effects of schema on memory. Specifically, our findings show that enhanced memory for more congruent information is mediated by the mPFC, which is hypothesised to guide integration of new information into a pre-existing schema represented in cortical areas, while memory for more incongruent information relies instead on automatic encoding of arbitrary associations by the MTL.

1. Introduction

It has long been known that relating new information to prior knowledge can enhance memory for that information, and this has been interpreted mainly in terms of facilitated retrieval via a pre-existing *schema* (Anderson, 1981; Bartlett, 1932; Bransford, Brown, & Cocking, 2000; DeWitt, Knight, Hicks, & Ball, 2012). More recently, the neural correlates of memory facilitation through activation of such schema have been found during both encoding (Tse et al., 2011; van Kesteren, Fernandez, Norris, & Hermans, 2010) and consolidation (Tse et al., 2007; van Kesteren, Rijpkema, Ruiter, & Fernandez, 2010; Wang & Morris, 2010), involving a functional interplay between the medial temporal lobe (MTL) and the medial prefrontal cortex (mPFC). From this neuroscientific perspective, a schema can be defined as a network of strongly-interconnected cortical representations, activation of which affects the processing of new, related information. Activated schemas are therefore presumed to facilitate all mnemonic stages: encoding, consolidation (e.g., through reactivation during offline periods such as sleep), and retrieval.

However, the specific roles of mPFC and MTL in this schema-dependent processing remain unclear. According to one recent theoretical framework (van Kesteren, Ruiter, Fernandez, & Henson, 2012), mPFC and MTL reflect distinct, complementary learning systems in the brain, whose relative influence on encoding depends on the congruency of new information with existing

* Correspondence to: Radboud University Nijmegen, Donders Institute for Brain, Cognition and Behaviour, Centre for Cognitive Neuroimaging, P.O. Box 9101, 6500 HB, Nijmegen, The Netherlands. Tel./Fax: +31 24 36 10980.
E-mail address: marlieke.vankesteren@donders.ru.nl (M.T.R. van Kesteren).
[1] Authors contributed equally.

0028-3932/$ - see front matter © 2013 Elsevier Ltd. All rights reserved.
http://dx.doi.org/10.1016/j.neuropsychologia.2013.05.027

schemas. This framework, termed *Schema-Linked Interactions between Medial prefrontal and Medial temporal regions* (SLIMM) proposes that, when new information is perceived that is congruent with a schema, a coherent pattern of mutually-reinforcing activity arises across the cortical network associated with that schema. This resonating network drives activity within mPFC, which is then assumed to directly augment cortical plasticity, thereby facilitating the integration of new information with the pre-existing schema. This contrasts with conventional accounts that only MTL can rapidly learn new associations (Scoville & Milner, 1957; Squire & Alvarez, 1995), but is consistent with recent evidence that such "cortical fast mapping" is possible in the presence of schema (Sharon, Moscovitch, & Gilboa, 2011). Furthermore, the increased mPFC activity is assumed to inhibit activity within the MTL, preventing simultaneous encoding of the new information by MTL. Only when the new information is not congruent with a dominant schema is the MTL able to encode that information, for example via indirect associations between hippocampal indices and the cortical representations activated by the new information (Marr, 1970; Murre, 1996); see (van Kesteren, et al., 2012) for further details.

We designed an fMRI experiment to test predictions of the SLIMM framework. We scanned participants while they rated the degree of congruency of visual images of an object and a scene, and used these ratings to define three levels of subjective congruency for each participant (i.e, congruency was defined on an individual basis). On the day after their scan, each participant was presented with objects only, and asked to distinguish "old" objects they had seen on the previous day from new ones (item recognition), and then, for the correctly remembered old objects, to indicate which of three alternative words described the scene that had been paired with that object on the previous day (associative recognition). This allowed us to return to the fMRI data during encoding of the object–scene pairs, and distinguish trials according to whether the association was subsequently remembered or forgotten to determine brain activity associated with successful associative encoding, as a function of the congruency of the pairing. If the SLIMM framework is correct, mPFC activity related to successful encoding should increase with congruency, while MTL encoding-related activity should decrease with congruency. Furthermore, functional connectivity between mPFC and parts of the ventral visual stream that code the objects and scenes should also increase with congruency (reflecting stronger binding via a schema), while functional connectivity between mPFC and MTL should also be modulated by congruency (van Kesteren et al., 2012).

2. Methods

2.1. Participants

Thirty-two native Dutch right-handed students (five male) participated in this experiment. All participants reported to be healthy, had normal or corrected-to-normal vision and were paid for their participation. Ethical approval was obtained from the institutional review board (CMO Region Arnhem-Nijmegen, The Netherlands), and all participants gave written informed consent. Four participants were excluded due to technical failure. Two other participants were excluded, because their behavioural performance did not yield a minimum of 9 trials for all categories included into contrasts of interest in the fMRI data analyses. Therefore, the data of these six participants were discarded and all analyses were performed on data of the remaining 26 participants (four male, age 18–27 years, mean 21.5 years). On average, participants reported to have slept 7.6 h the night in between the two experimental days (range 6.5–9 h).

2.2. General procedure

Participants performed an associative memory experiment, conforming to a 3×2 (congruency $\times$ memory) factorial design. Inside the scanner, on day one, they rated the congruency of, and intentionally memorised, 185 sequentially presented paired associates, each consisting of two colour photographs simultaneously presented next to each other, one scene and one object (Fig. 1). The congruency ratings, performed on a 33-point scale that appeared continuous to the participants, were subsequently used to divide the stimuli into three congruency levels of identical trial counts (congruent, intermediate and incongruent). Before the encoding task, participants underwent a functional localiser experiment that lasted about ten minutes and after the encoding task, which lasted about 25 min, an anatomical scan was acquired, which lasted seven minutes. Participants then went home and returned the next day, approximately 24 h later, when their memory was tested with an object recognition test and an object–scene associative memory test, which were administered outside the MR scanner.

2.3. Stimuli

Participants were instructed to memorise 185 paired-associates each consisting of two colour photographs, one scene and one object. We used both indoor- and outdoor-scenes (e.g. classroom, tennis court) which were easily recognisable and could be distinctively described by one or two words (as assessed in a pilot study, see Section 2.4). Pairs were predefined, such that object–scene associations would cover the whole range of the congruency scale and were unique, i.e. each picture was shown in only one pair. Ten per cent of the pairs were constructed to be very incongruent (e.g. tennis court–soup ladle), while another 10% were constructed to be very congruent (e.g. classroom–chalk). To most optimally counterbalance the design across participants, for half of the participants, the objects that were paired as very congruent before were re-paired within their subset to give very incongruent combinations, while the objects that were paired as very incongruent for the first half of participants were re-paired within their subset to give very congruent combinations. Thus, 20% of the objects and scenes were shown in either a very congruent or a very incongruent pairing, counterbalanced across participants, to control for biases resulting from our construction of the pairs. Consequently, 80% of the pairs were likely to be rated as more intermediately congruent, allowing subjective congruency ratings to be widely distributed.

2.4. Behavioural pilots

Prior to conducting the associative memory experiment in the MR scanner, we performed four behavioural pilots in a separate group of participants ($n=26$ in total). In these, we checked whether the pictures were easy to recognise and to describe and whether congruency of the constructed pairs fitted the intended distribution across the congruency scale (see Section 2.5). During piloting we also confirmed that the number of trials was appropriate to attain behavioural performance above chance level while keeping enough trials in all conditions for our MR-analyses.

2.5. Associative memory encoding

The experiment was executed on two consecutive days (Fig. 1). On the first day, participants were instructed to memorise the 185 pairs while brain activation was measured using fMRI. Participants lay in the MR scanner supine and viewed the screen through a mirror mounted on the head coil while they responded with their right index and middle finger using a button box. Presentation 14.9 (NeuroBehavioural Systems Inc., Albany, CA, USA) was used to present the stimuli. Participants were instructed to remember the pairs for a test 24 h later, but were not told what aspects they would be tested on. During the encoding task, the object and scene picture making up a pair were presented simultaneously and next to each other on a grey background for 3.5 s, followed by an intertrial interval of 2–6 s duration, during which a black fixation cross on grey background was shown. Pairs were presented pseudorandomly, with no more than three very congruent or very incongruent items following each other. All items (objects and scenes) were presented on two screen locations left and right of the centre. The side of the object and scene on screen (left or right) was randomized across trials. Additionally, 12 baseline periods of 10 s were interspersed evenly, during which a black fixation cross on grey background was shown. Due to technical problems, all durations were scaled by a factor of 1.5 for one participant, but because her results did not deviate we included her data in the analysis. During pair presentation, participants had to judge the congruency of the pair by moving a red bar acting as cursor on a visual analogue scale (which was in fact a discrete scale with 33 parts that were not discernible for the participants), labelled on one end as *does not fit*, in the middle as *possible* and on the other end as *fits very well* (Fig. 1). The left/right orientation of the scale (*well* $<>$ *not well* or *not well* $<>$ *well*) was counterbalanced across participants.

Twenty-four hours later (standard deviation (SD) 1 h), participants returned for the memory test (Fig. 1). On a computer screen, they were shown a set of 300 object pictures, consisting of the 185 pictures from day one as well as 115 new pictures that served as lures. These objects were not directly paired with learned objects, but were somewhat related to make the recognition task less easy. Participants were instructed to decide whether they had seen these objects the

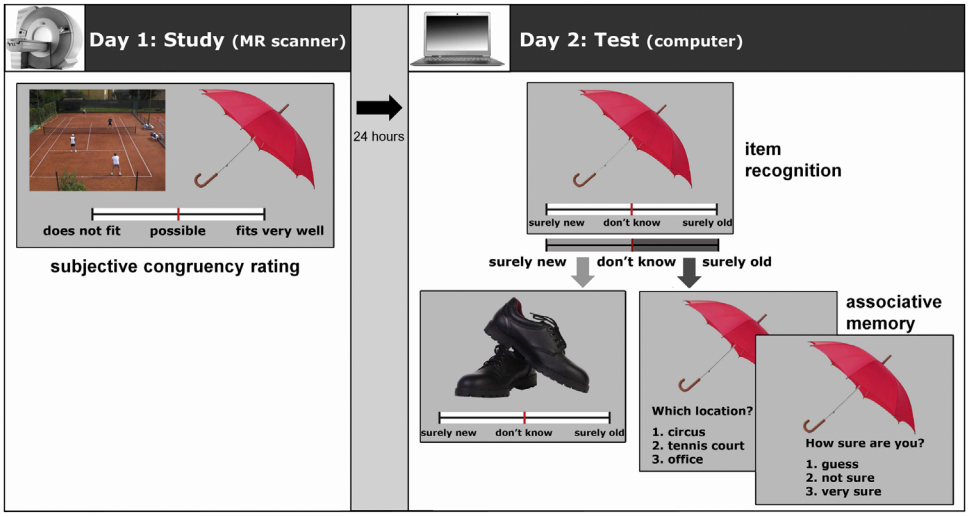

Fig. 1. Experimental design. The experiment was conducted on two consecutive days. On day one, participants memorised a series of consecutively presented pairs of photographs in the MR scanner. Each pair of photographs contained one object and one scene, and participants were asked to indicate how well they thought the two photographs matched in terms of their co-occurrence in the real world, by moving the red bar on a congruency scale to a particular position. These ratings were used to assess subjective congruency, and then split into thirds to define three levels of participant-specific congruency. Participants returned 24 h later to be tested on their memory. Participants were shown old and new object photographs sequentially and randomly intermixed, and indicated whether they had seen the object the previous day by moving the red bar on a confidence scale (item recognition). For objects judged as old, they were subsequently asked to choose one of three one-word descriptions of scenes that corresponded to the scene paired with the object on the previous day (associative memory). Finally, they were asked to rate their confidence on this decision (guess, not sure, very sure). Participants had to answer each question within six seconds.

previous day by moving a red bar on a visual analogue scale (which was the same scale as used in the encoding experiment, see above), labelled on one end as *surely new*, in the middle as *don't know*, and on the other end as *surely old*. For items judged as old, participants had to indicate which scene was associated to it, choosing from three one-word descriptions. We used verbal descriptions instead of the original scene pictures to make the test harder and to eliminate recognition from idiosyncratic perceptual features of the photographs; instead testing more categorical-type memories. One correct answer and two other scenes from the studied set were provided in the three-choice question. To avoid the possibility of identifying the correct answer by solely remembering that the object had been shown with a congruent or incongruent scene, multiple choice options were manually arranged to have, additional to the correct answer, both one congruent and one incongruent incorrect option. All scenes were distributed to appear equally often as an option. Lastly, participants had to indicate how confident they were of their answer (three choices: *guess*, *not sure*, and *very sure*). Each response had to be given within six seconds, after which the next question was shown.

2.6. Localiser experiment

To determine brain regions that represent objects and scenes, a functional localiser experiment for objects and for scenes was conducted before the encoding task. Participants were shown colour photographs of objects, natural scenes, scrambled objects and scrambled scenes in a blocked design. The photographs used in the localiser experiment were different from the ones used in the associative memory experiment. Participants saw the same set of 24 pictures for each stimulus type five times, equalling 20 blocks with a total of 480 stimulus presentations. Blocks were presented in the same pseudo-random order for each participant. Each picture was presented for .7 s, followed by an intertrial interval of .4 s duration, during which a grey background was shown. During the localiser experiment, participants performed a 1-back task. They were instructed to press a button if the same picture appeared twice consecutively. Participants were told that they would not have to remember the pictures shown during the localiser task.

2.7. Behavioural analyses

According to the congruency ratings given on day one, study phase trials were grouped into three congruency bins with approximately identical trial numbers labelled congruent, intermediate, and incongruent. Trials in which no congruency rating was given, i.e. the red bar was not moved, were excluded from the analysis. Reaction times were defined in two measures. First, we used the time it took participants to decide how congruent they thought a particular pair was (decision time), reflected in the time it took them to start giving a response, i.e. the duration from the onset of pair presentation until initiation of the answer. Second, we calculated the duration of the actual response (response time), i.e. the duration from the first until the last button press within a trial. The response time was necessarily related to a pair's congruency level, as the red bar was positioned in the middle of the scale at the beginning of each trial and had to be moved further towards the ends of the scale for more incongruent or congruent judgments, resulting in longer response times. By combining these two measures, we also calculated the overall reaction time per trial.

In the second day memory test, all responses on the object recognition question from scale part 1 (surely new) to 15 were classified as *new* answers, while all responses from scale part 19 to 33 (surely old) were classified as *old* answers, leaving out the intermediate (don't know) answers and the trials where the cursor was not moved. All trials with intermediate scores, i.e. scale parts 16 to 18, were discarded from the analysis, to exclude trials in which no choice had been made, i.e. the red bar had not been moved, as well as the adjacent very unsure decisions. Item recognition performance (*d*-prime) for each congruency level was then calculated as the *z*-transformed proportion of objects in each congruency bin included in the analysis that were correctly identified minus the *z*-transformed proportion of false alarms. Subsequently, associative memory performance was calculated as the proportion of correctly recognised objects for which the scene was correctly identified, irrespective of the associative memory confidence.

To analyse the behavioural measures, PASW Statistics 18 (SPSS Inc., Chicago, IL, USA) was used. Student's *t*-tests were performed to assess whether memory scores differed from chance level (one-sample *t*-tests against 0 for item recognition accuracy and .33 for associative memory performance) and whether memory scores, reaction times, beta weights (see below), and confidence of associative memory differed between congruency levels (paired-sample *t*-tests). For this purpose, the verbal confidence ratings of associative memory answers were transformed to an ordinal representation by scoring *guess* as 1 point, *not sure* as 2 points, and *very sure* as 3 points. To assess whether scores changed consistently across congruency levels, we ran repeated-measures analyses of variance (ANOVAs), testing for monotonic trends in the data. All measures were considered significant at a threshold of alpha = .05.

2.8. fMRI data acquisition

Participants were scanned using a 1.5 T Siemens Magnetron Avanto system equipped with a 32 channel phased-array head-coil (Siemens AG, Erlangen, Germany). For blood-oxygen level dependent (BOLD) fMRI images, we used a T2*-weighted, gradient-echo, multi-echo EPI sequence (Poser, Versluis, Hoogduin, & Norris, 2006) with the following parameters: repetition time (TR) = 2.64 s, echo time (TE)1 = 6.9 ms, TE2 = 24.2 ms, TE3 = 33 ms, TE4 = 43 ms, TE5 = 52 ms, 34 slices, ascending slice order, 3 mm slice thickness, .51 mm slice gap, matrix size = 64 × 64, field of view (FOV) = 224 × 224 × 199 mm, flip angle = 80 degrees, voxel size = 3.5 × 3.5 × 3.0 mm. Slices were angled in an oblique axial manner to achieve whole brain coverage. To allow T1 saturation to reach equilibrium, the first three volumes were discarded. Additionally, T1-weighted anatomical scans at 1 mm isotropic resolution were acquired using an MPRAGE scan with TR = 2250 ms, inversion time (TI) = 850 ms, flip angle = 15 degrees and FOV = 350 × 263 × 250 mm.

2.9. fMRI data preprocessing

For both encoding task and localiser experiment, raw multi-echo fMRI data were first processed using in-house software written in Matlab 7.5 (The Mathworks, Inc., Natick, MA, USA), which used 32 separately acquired scans to calculate the optimal weighting of echo times for each voxel (i.e. by using a weighted measure of the contrast- to-noise ratio for each echo/scan). Motion correction was performed on the first echo by using iterative rigid body realignment to minimise the residual sum of squares between the first and all further functional images. Then the calculations of optimal echo time for each voxel were used to combine multi-echo fMRI data into single-echo images. The combined images were further processed using SPM8 (http://www.fil.ion.ucl.ac.uk/spm). Functional images were realigned to a mean functional image, and coregistered to the corresponding individual anatomical scan by using mutual information optimisation. These images were subsequently spatially normalised and transformed to a common space, as defined by the SPM8 Montreal Neurological Institute (MNI) T1 template (voxel size = 2 × 2 × 2 mm), as well as spatially smoothed by convolving them with an 8 mm full width at half maximum 3D kernel.

2.10. fMRI data analysis

2.10.1. Localiser experiment

The blocked design of the localiser experiment yielded four conditions (objects, scenes, scrambled objects, and scrambled scenes), which we modelled by convolving the block durations with a canonical haemodynamic response function. In a general linear model (GLM), we included these four conditions and six motion parameters. We entered these statistical maps into a full factorial second level analysis (type × scrambling), and then calculated object (objects–scrambled objects) and scene (scenes–scrambled scenes) contrasts. Statistical maps for the localiser experiment were analysed at a threshold of voxel level $p < .05$ whole-brain family-wise error (FWE) corrected.

2.10.2. Encoding task

According to the behavioural outcome from the retrieval test, we classified study phase trials as item misses (object not recognised), item hits (object recognised but associated scene incorrect) and associative hits (item recognised and associated scene correct) for each of the three congruency levels. For each level, trial categories were modelled by convolving a boxcar function of pair presentation duration (3.5 s) with a canonical haemodynamic response function. In a GLM, we included these nine trial types, the baseline trials and six motion parameters. Additionally, we included decision time (the duration from the onset of the presentation of a new pair until the first button press within a trial) and response time (time from first button press until last button release within a trial) as parametric modulators for all trials, and confidence of associative hits (1, 2, or 3 points) as parametric modulators for associative hits only, forming a design matrix with 38 regressors.

For the main encoding phase, we focused on regions of interest (ROI) defined either on the basis of previous studies, or on the independent localiser data. More specifically, we report any peak within an ROI whose statistic exceeded $p < .05$ corrected for family-wise-error (FWE) using small-volume correction (SVC) within each ROI (see below). For completeness, we also report any other clusters (outside these ROIs) whose extent (defined by an statistical threshold of $p < .001$ uncorrected) survived p(FWE) < .05 corrected for the whole brain. The ROI for the mPFC was defined functionally, using an 8 mm sphere centred on the peak voxel (MNI [2,46,0]) in mPFC for the contrast of congruency × cued recall in our previous study (van Kesteren, Rijpkema, Ruiter, & Fernandez, 2011). The ROIs for ventral temporal cortical regions assumed to represent the current stimuli and used in the connectivity analysis (see hypotheses in Introduction) were derived from the independent functional localiser data of the present study; specifically, the peaks from the contrasts of scenes versus scrambled scenes, and objects versus scrambled objects in lateral occipital cortex (LOC) and parahippocampal place area (PPA) (see Results), were used as the centres of spheres with a radius of 20 mm. Finally, the ROIs for the MTL were derived anatomically, from combining the Automatic Anatomic Labelling (AAL) definitions of the hippocampus and parahippocampal gyrus (Tzourio-Mazoyer et al., 2002), separately in left and right hemispheres. All brain coordinates are given in MNI space.

2.10.2.1. Activity analysis. We calculated a subsequent memory contrast as the difference between associative hits and misses (the average of item hits and item misses), separately for each congruency level, within each participant. Subsequently, we entered the resulting contrast images into a multiple regression which included two regressors: a mean and linear function of congruency. The mean regressor therefore tested for the main effect of subsequent associative memory across participants, while the (orthogonal) linear regressor tested the interaction between subsequent memory and congruency (we also looked for a quadratic component in separate analyses, but nothing survived correction for our ROIs). This linear effect of congruency was tested either in the direction of *congruency*, i.e. linearly increasing from incongruent to intermediate to congruent, or in the direction of *incongruency*, i.e. linearly decreasing with increasing congruency. Beta weights for each original condition from the peak of the significant clusters identified by the above model were extracted using in-house software written in Matlab 7.11 (The Mathworks, Inc., Natick, MA, USA).

2.10.2.2. Functional connectivity analysis. We computed psycho–physiological interactions (PPI), using two seed regions: a sphere with a radius of 8 mm centred at the peak voxel in mPFC (MNI [−2,40,2]), which showed a positive interaction between memory and congruency in the activity analyses, and a cluster in left MTL which showed a negative interaction between memory and congruency, consisting of 51 voxels that survived $p < .001$ uncorrected (see Results). Note that changes in connectivity are not necessarily related to changes in mean activity, so this selection of ROIs based on experimental effects on activity does not bias the connectivity results (Friston et al., 1997). Separately for all congruency levels, we computed the connectivity of the seed region with all other voxels, testing for regions that showed an interaction between the time course of the seed region's BOLD response (physiological variable) and the subsequent memory contrast for each of the three congruency levels, as used in the activity analyses (psychological variable). The resulting contrast images, indexing regions whose connectivity with the seed was stronger for hits than for misses for a given congruency level, were entered into further multiple regression analyses, again probing an increase or decrease with congruency as described above. Hence, we tested for regions whose change in connectivity associated with hits versus misses varied with increasing or decreasing congruency.

3. Results

3.1. Behavioural measures

3.1.1. Item recognition accuracy

Item recognition accuracy (d-prime, Fig. 2A) was above chance level (0) for all congruency levels (incongruent pairs: $t(25) = 18.19$, $p < .001$; intermediate pairs: $t(25) = 16.99$, $p < .001$; congruent pairs: $t(25) = 20.32$, $p < .001$). Item recognition measures increased linearly with congruency (linear component: $F(1,25) = 15.37$, $p = .001$; quadratic component: $F(1,25) = 3.61$, p = n.s.). Items from congruent pairs were better remembered than items from incongruent pairs ($t(25) = 3.92$, $p = .001$) and intermediate pairs ($t(25) = 3.79$, $p = .001$). Item recognition accuracy of incongruent and intermediate pairs did not differ significantly ($t(25) = .35$, p = n.s.).

3.1.2. Associative memory performance

Associative memory performance (proportion correct, Fig. 2B) was above chance level (33%) for all congruency levels (incongruent pairs: $t(25) = 7.79$, $p < .001$; intermediate pairs: $t(25) = 13.77$, $p < .001$; congruent pairs: $t(25) = 21.67$, $p < .001$). Associative memory performance increased monotonically with congruency (linear component: $F(1,25) = 46.08$, $p < .001$, quadratic component: $F(1,25) = 8.9$, $p < .01$) and differed significantly between all three levels (intermediate pairs–incongruent pairs: $t(25) = 2.50$, $p < .05$; congruent pairs–intermediate pairs: $t(25) = 7.13$, $p < .001$; congruent pairs–incongruent pairs: $t(25) = 6.79$, $p < .001$).

3.1.3. Confidence measures

Confidence increased monotonically with congruency for item recognition hits (1–33); linear component: $F(1) = 23.94$, $p < .001$; quadratic component: ($F(1,25) = 8.64$, $p < .01$). For associative recognition, confidence (minimum 1 point, maximum 3 points) showed a significant linear increase with congruency, averaging across hits and misses (linear component $F(1,25) = 37.80$, $p < .001$; quadratic component: $F(1,25) = 1.11$, p = n.s.), but any interaction between memory (hits vs misses) and congruency failed to reach significance ($F(2,24) = 2.47$, p = n.s.).

3.1.4. Reaction times

Reaction times during encoding showed a linear decrease with congruency (linear component: $F(1,25) = 47.46$, $p < .001$; quadratic component: $F(1,25) = 1.28$, p = n.s.) Congruent trials showed significantly faster reaction times than intermediate ($t(25) = 3.15$, $p < .01$) and

incongruent trials ($t(25)=6.89$, $p<.001$). Reaction times for incongruent and intermediate trials did not differ significantly ($t(25)=1.03$, $p=$n.s.). However, because the participants performed a congruency rating on a scale where the cursor always started in the middle and was moved by a series of button presses, the reaction times can be divided into two parts: decision times (duration from the beginning of a pair presentation until the first button press within a trial) and response times (duration from the first to the last button press within a trial). As this measure is differentially affected by congruency due to the nature of the experiment (intermediate trials require less response times as the cursor always starts in the middle), we examined these two types of reaction time separately. Decision times differed significantly between congruency levels (incongruent pairs: mean=1.66 s, SEM=.04 s; intermediate pairs: mean=1.99 s, SEM=.06 s; congruent pairs: mean=1.57 s, SEM=.04 s; linear component: $F(1,25)=14.63$, $p=.001$; quadratic component: $F(1,25)=214.32$, $p<.001$), as did response times (incongruent pairs: mean=.78 s, SEM=.03 s; intermediate pairs: mean=.41 s, SEM=.04 s; congruent pairs: mean=.71 s, SEM=.03 s; linear component: $F(1,25)=7.73$, $p=.01$; quadratic component: $F(1,25)=115.88$, $p<.001$).

3.2. Brain activity

3.2.1. Localiser contrasts

The localiser experiment revealed distinct, bilateral brain regions that were more strongly activated during processing of objects and scenes, respectively (see Fig. 5). Activity in fusiform gyrus and LOC (peaks [−48,−78,2], [48,−70,−4]) was enhanced bilaterally in response to objects. Activity in the PPA was enhanced bilaterally in response to scenes (peaks [−26,−48,−8], [24,−40,−12]) (Fig. 5A, C). We used these results for small-volume correction of the connectivity analyses below (see Methods).

3.2.2. Main effect of subsequent associative memory

The contrast of greater activity for associative hits than misses revealed a main effect of subsequent memory, regardless of congruency, in left MTL (hippocampus; [−30,−16,−12]) $p(SVC)<.05$ (Fig. 3; and Table S1), left inferior frontal cortex, left fusiform cortex, left mid occipital cortex and left frontal inferior triangle ($p<.05$ whole-brain cluster-level corrected).

3.2.3. Interaction between subsequent memory and congruency

We first tested for regions in which the subsequent memory effect increased (linearly) with congruency. Using our a priori mPFC ROI (based on our previous study, see Methods) the peak statistic at [−2,40,2] survived correction, $p(SVC).<05$ (Fig. 4A and C; but also see Fig. S1A; Table S2). The opposite test for regions in which the subsequent memory effect decreased with congruency revealed no significant effects at whole-brain level, but a peak in left parahippocampal cortex ([−16,−18,−20]) survived correction for our left MTL ROI, $p(SVC).<05$ (Fig. 4B and D; but also see Fig. S1B; Table S2). Only one mid-cingulate cluster survived $p<.05$ whole-brain cluster-level correction. Thus mPFC, as well as cingulate regions, showed activation associated with successful associative encoding that increased with the congruency of the association, whereas MTL showed encoding-related activation that decreased with the congruency of the association (i.e. that was greatest for incongruent pairs).

3.2.4. Functional connectivity

To investigate how connectivity of the areas shown to be involved more strongly with the encoding of either congruent (mPFC) or incongruent (left parahippocampal) pairs differed across congruency levels, we ran psycho–physiological interaction (PPI) analyses. These tests revealed a peak within the right PPA ROI defined from the localiser, whose connectivity from the mPFC increased with increasing congruency during successful associative encoding ([12,−38,−8], $p(SVC)<.05$) (Fig. 5). When testing for the opposite contrast, we found decreased connectivity with increasing congruency from mPFC to more dorsal medial prefrontal regions, and to an angular gyrus region, that survived whole-brain cluster-level correction. No voxel survived SVC for this contrast in our ROIs, though a hippocampal peak within our right MTL ROI ([32,−28,−6]) showed a trend, p(SVC)=.075. Finally, when testing for connectivity from the left parahippocampal seed, we did not observe significant interactions in the whole-brain or in our ROIs.

4. Discussion

In this experiment, we investigated how brain activity during encoding of new associations is altered as a function of the subjective congruency of those associations with pre-existing schemas. The results replicate and extend earlier findings on schema effects during memory encoding (Tse, et al. 2011; van Kesteren, Fernandez et al., 2010; van Kesteren et al., 2011), by using subjectively-defined congruency levels, and provide support for some of the predictions made by the recent SLIMM framework (van Kesteren et al., 2012). We explore these predictions in turn.

Behaviourally, we found that item recognition increased linearly and associative recognition increased monotonically across

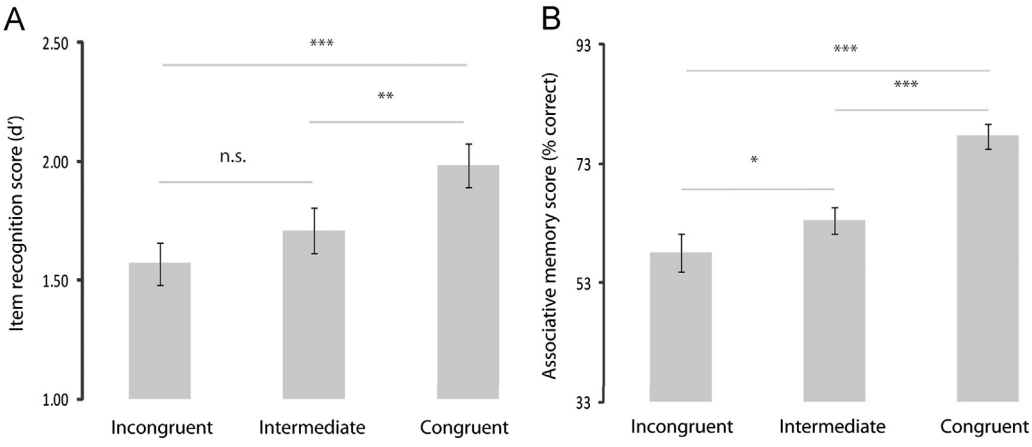

Fig. 2. Memory performance. (A) Mean (and SEM) of item recognition accuracy (d-prime) for each congruency level. (B) Mean (and SEM) of associative recognition performance (% correct) for each congruency level. Smaller horizontal bars indicate post-hoc paired-samples *t*-tests between two congruency levels; $^{*}p<.05$; $^{**}p<.01$; $^{***}p<.001$; n.s. $p>.05$. SEM: standard error of the mean.

our three levels of congruency (Fig. 2), consistent with previous data on the memory advantage for congruent information (Bransford & Johnson, 1972; Staresina, Grey, & Davachi, 2009; van Kesteren, Rijpkema et al., 2010; van Kesteren et al., 2011). Confidence levels also increased linearly with congruency for both memory measures.

Consistent with earlier neuroimaging findings (Paller & Wagner, 2002; Tendolkar et al., 2007), main effects of subsequent associative memory (Fig. 3), averaging across congruency, were found in regions including the left hippocampus, left inferior frontal gyrus and left fusiform gyrus. The interaction between subsequent memory and congruency, on the other hand, revealed encoding-related activity in mid and posterior cingulate cortex that increased with congruency (Fig. 4A). These activations are often reported in memory retrieval tasks (Huijbers, Pennartz, Rubin, & Daselaar, 2011; Sugiura, Shah, Zilles, & Fink, 2005; Wagner, Shannon, Kahn, & Buckner, 2005), and so this interaction may reflect congruent pairs, by their nature, having greater retrieval of associated information than less congruent pairs. More importantly, as predicted, mPFC also showed encoding-related activity that increased linearly with subjective congruency. This interaction is consistent with the SLIMM framework (van Kesteren et al., 2012), in which mPFC is assumed to respond to the degree of resonance within cortical networks, and representations of congruent information will resonate more. This increased mPFC activity is then assumed to facilitate plasticity between the representations within those networks, enhancing later associative memory.

SLIMM also predicts that mPFC activity inhibits activity within MTL, and therefore MTL activity will show the opposite pattern, of increased activity with decreasing levels of congruency. This prediction was also confirmed, at least within a left parahippocampal region within our MTL ROI (Fig. 4B). This finding is also consistent with previous studies that found subsequent associative memory effects in parahippocampal cortex for tasks that required participants to learn arbitrary associations (Staresina, Duncan, & Davachi, 2011; Tendolkar et al., 2007), which are analogous to the less congruent conditions of in the present design. Nonetheless, there are also data suggesting that successfull encoding of congruent information relates to enhanced processing in hippocampus (Staresina et al., 2009). We acknowledge these results that appear inconsistent with SLIMM. Nonetheless, there are several procedural differences between that study and ours (e.g., incidental vs intentional learning, same day vs next day testing, colour-word vs object-scene associations) that might account for these differences, and could be explored in future studies. We also acknowledge that regions observed in the main effect are not present in the interaction results. These null effects are likely to be a power issue (which could be addressed in future research). Regardless, the critical interaction we tested is significant and is thus a first step towards unpacking the precise relationship between subsequent memory and congruency in future work.

Furthermore, SLIMM predicts that the facilitation of cortical learning for schema-consistent information by mPFC is associated with increased functional connectivity between mPFC and the cortical regions that represent that information. In the present experiment, we used a localiser scan to identify a PPA ROI that was activated by our scene stimuli (where the PPA lay posterior to our anatomically-defined MTL ROI), and an LOC ROI activated by our object stimuli. Consistent with SLIMM's predictions, we found that connectivity from mPFC to PPA increased with increasing congruency (Fig. 5), suggesting that mPFC was influencing encoding-related activity associated with the scene stimuli (though we did not find this increased connectivity to the LOC ROI associated with the object stimuli). These results extend our previous finding of enhanced functional connectivity from the mPFC to a task-relevant somatosensory cortical area during retrieval of congruent information (van Kesteren, Rijpkema et al., 2010), in showing that functional connectivity between mPFC to such sensory representational areas is augmented by schemas during encoding, too.

Finally, SLIMM also predicts changes in connectivity between mPFC and MTL as a function of congruency, associated specifically with an inhibition of MTL activity by mPFC for congruent information. However, how this inhibitory account translates into changes in functional dependencies between fMRI data remains unclear. Before, we argued that mPFC–MTL connectivity will in fact be greatest for intermediate levels of congruency, where there may only be partial activation of schemas, and hence of mPFC, so greater interaction between mPFC and MTL is necessary to resolve this "competition" (van Kesteren et al., 2012). We did not find evidence of this quadratic relationship across the present three levels of congruency. If anything, we found a trend for functional connectivity (from mPFC to a right hippocampal region) to increase linearly with decreasing congruency. This prediction therefore clearly requires further theoretical development (concerning how inhibitory interactions relate to fMRI connectivity measures) and further empirical data, specifically looking at mPFC–MTL connectivity with other, causal measures.

Note that we did not find any evidence of enhanced memory for incongruent information in this experiment. According to SLIMM, associations that are incongruent with a schema (i.e, highly novel) are encoded by an index (instance) in the MTL, and this "snapshot" should occur more often for low than for intermediate levels of congruency. Together with the aforementioned, mPFC-mediated advantage for highly congruent information, one might therefore expect a U-shaped function across the 3 levels of congruency used here. However, the prediction for behavioural performance also depends on the precise nature of the encoding and retrieval tasks, as discussed below.

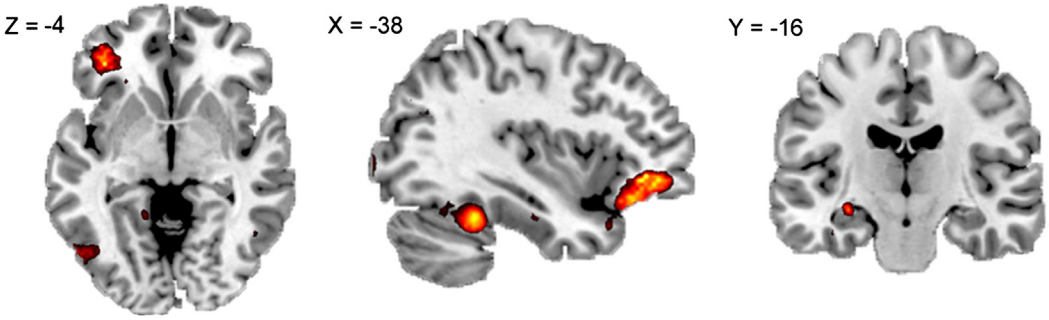

Fig. 3. Main effect of subsequent memory for object–scene associations. The contrast between associative hits and misses, averaged across congruency, revealed (amongst others) activation in left inferior frontal gyrus (left and middle panel), left fusiform gyrus (middle panel), and left hippocampus (peak [−30,−16,−12], right panel). All maps are shown at $p < .001$ uncorrected, and all clusters survived whole-brain correction for their spatial extent, or small volume correction for their peak within pre-specified ROIs (see Methods).

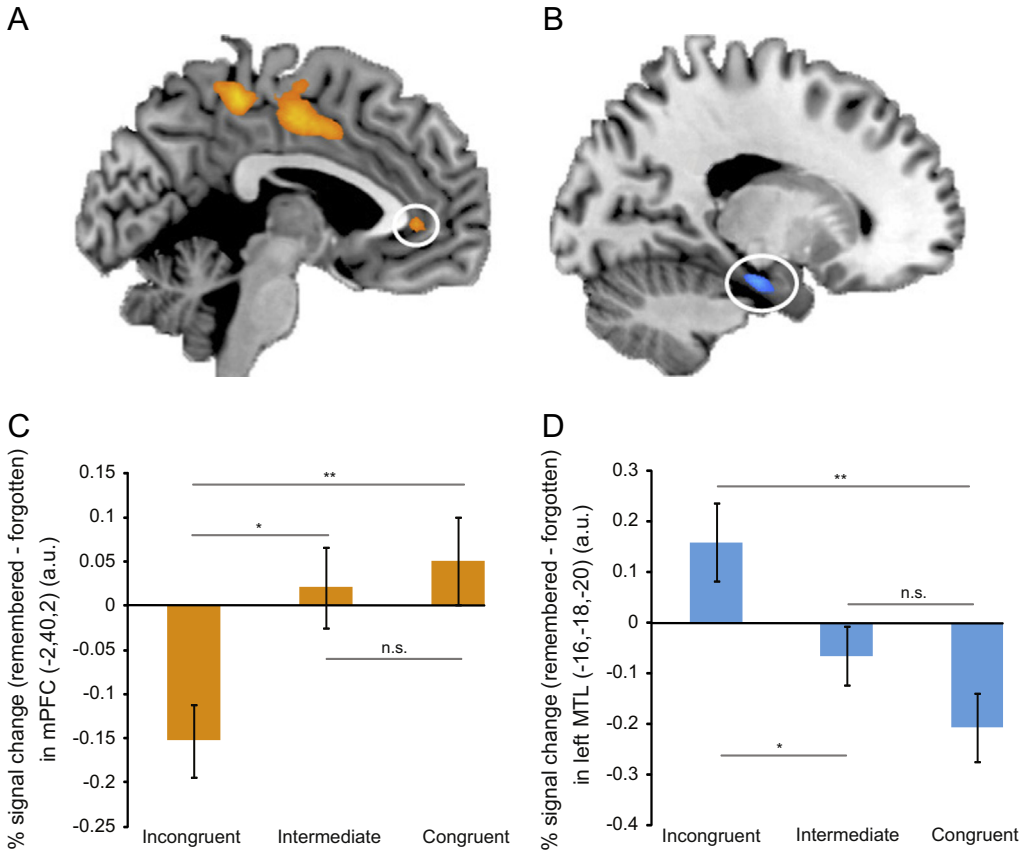

Fig. 4. Effects of congruency on subsequent associative memory. Statistical maps show the results of testing for brain regions that show an interaction between subsequent memory and congruency. Linear regression analyses were performed on the subsequent memory contrasts across the three congruency levels, either testing for an increase with congruency (A) or an increase with incongruency (B). (A) Encoding-related activity in the medial prefrontal cortex (mPFC) ROI increased with congruency (peak [−2, 40, 2]). (B) Encoding-related activity in the left medial temporal lobe (MTL) ROI increased with incongruency (peak [−16,−18, 20]). (C) Mean (+/− SEM) of the subsequent memory contrast for each level of congruency extracted from the mPFC peak (A). (D) Mean (+/− SEM) of the subsequent memory contrast for each level of congruency extracted from the MTL peak (B). Maps displayed at $p < .005$ uncorrected for the purpose of illustration. Peaks in mPFC and MTL are significant after small-volume correction for their respective ROIs, while the extent of the mid and posterior cingulate clusters survives correction across the whole brain. (C+D) Horizontal bars indicate paired-samples *t*-tests between two congruency levels; $^{*}p < .05$; $^{**}p < .01$; n.s. $p > .05$ for illustrative purposes, since these *p*-values are biased by prior selection of the voxels to show a linear effect across all three congruency levels.

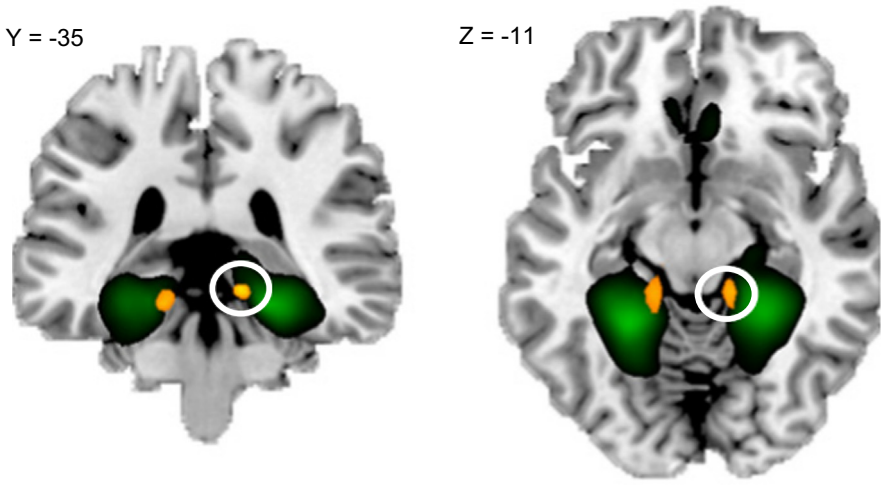

Fig. 5. Effects of congruency on functional connectivity during successful memory encoding. Statistical maps show the results of a linear regression of the interaction between connectivity of a seed region and subsequent memory for each congruency level, imposed on localiser experiment results (green: scene localiser). Connectivity of the mPFC with right parahippocampal place area during successful encoding increased with congruency (shown in yellow, peak [12,−38,−8], on top of scene localiser (green) $p(\text{FWE}) < .05$ in coronal and axial views). Map displayed at $p < .001$ uncorrected at voxel level. The left PPA was also activated at this whole-brain threshold but did not survive subsequent small volume statistics.

Foremost is the issue of a "generate-and-recognise" strategy at retrieval (Watkins & Gardiner, 1979), in which participants generate information from pre-existing schemas that is congruent with the retrieval cue (here, the picture of the object), and then detect whether such information seems familiar (recognised), as would occur if it had been paired with the cue at encoding. We tried to reduce the effectiveness of this strategy by using a forced-choice associative recognition test, in which names of three possible scenes were provided, so that participants need not generate possible scenes themselves. Additionally, we deliberately made one of the two incorrect choices match the (predefined) congruency level of the correct choice, so that merely remembering that an association was congruent or incongruent would not be sufficient to select the correct choice. Nonetheless, it remains possible that we could not fully prevent use of a generate-and-recognise strategy, which might have boosted performance for congruent trials, and masked any advantage for incongruent trials. Note however that this retrieval strategy would not directly affect the neuroimaging data at encoding, because the MTL could still show increased activity for remembered versus forgotten incongruent trials, even if this activity were not sufficient to overcome any retrieval bias towards congruent trials.

Secondly, a stronger test of MTL-encoding of incongruent items, according the SLIMM framework, would be to test memory for incidental associations that were not directly relevant to the encoding task (e.g, the left-right location of the object and scene). This is because the MTL is assumed to take an episodic "snapshot" of all information present at encoding, so such incidental context should be better remembered for incongruent than congruent trials (where an active schema, and active mPFC, is predicted to actually filter out such unrelated information (van Kesteren et al., 2012)). This is consistent with evidence that memory benefits for incongruent/unexpected information seem to generally arise under incidental encoding conditions (Kormi-Nouri, Nilsson, & Ohta, 2005; Tulving & Kroll, 1995), and particularly affect task-irrelevant contextual and perceptual details (as e.g. in Davis, Love, and Preston (2012)). Because participants in our study were aware that their memory would be tested later, they will have deliberately focused on trying to relate the object and scene, meaning that the scene memory targeted by our recognition test was not incidental. Future research should focus more specifically on testing task-irrelevant, incidental features of incongruent memories.

In conclusion, the present study revealed that the subjective congruency of new information with prior knowledge affected subsequent memory performance, activity in mPFC and MTL and functional connectivity between mPFC and sensory regions. These results provide support for the SLIMM framework, which proposes that two distinct neural mechanisms, instantiated in mPFC and MTL, interact during memory encoding, where the extent to which each contributes to encoding is governed by the congruency of the learned information with a pre-existing schema. Future research should focus on further specifying features of congruent and incongruent memory traces during and after encoding.

Acknowledgments

This work was supported by grants from RUNMC (RG000457), the European Research Council (ERC-2010-AdG 268800-NEUROSCHEMA), the UK Experimental Psychology Society, and the UK Medical Research Council Program.

Appendix A. Supporting information

Supplementary data associated with this article can be found in the online version at http://dx.doi.org/10.1016/j.neuropsychologia.2013.05.027.

References

Anderson, J. R. (1981). Effects of prior knowledge on memory for new information. *Memory and Cognition*, *9*(3), 237–246.
Bartlett, F. C. (1932). *Remembering: A study in experimental and social psychology*. Cambridge, [England]: University Press.
Bransford, J. D., Brown, A. L., & Cocking, R. R. (2000). *How people learn: brain, mind, experience and school*. Washington D.C.: National Academy Press.
Bransford, J. D., & Johnson, M. K. (1972). Contextual prerequisites for understanding—some investigations of comprehension and recall. *Journal of Verbal Learning and Verbal Behavior*, *11*(6), 717–726.
Davis, T., Love, B. C., & Preston, A. R. (2012). Learning the exception to the rule: Model-based FMRI reveals specialized representations for surprising category members. *Cerebral Cortex*, *22*(2), 260–273.
DeWitt, M. R., Knight, J. B., Hicks, J. L., & Ball, B. H. (2012). The effects of prior knowledge on the encoding of episodic contextual details. *Psychonomic Bulletin and Review*, *19*(2), 251–257.
Friston, K. J., Buechel, C., Fink, G. R., Morris, J., Rolls, E., & Dolan, R. J. (1997). Psychophysiological and modulatory interactions in neuroimaging. *Neuroimage*, *6*(3), 218–229.
Huijbers, W., Pennartz, C. M., Rubin, D. C., & Daselaar, S. M. (2011). Imagery and retrieval of auditory and visual information: Neural correlates of successful and unsuccessful performance. *Neuropsychologia*, *49*(7), 1730–1740.
Kormi-Nouri, R., Nilsson, L. G., & Ohta, N. (2005). The novelty effect: Support for the novelty-encoding hypothesis. *Scandinavian Journal of Psychology*, *46*(2), 133–143.
Marr, D. (1970). A theory for cerebral neocortex. *Proceedings of the Royal Society of London B: Biological Science*, *176*(43), 161–234.
Murre, J. M. (1996). TraceLink: A model of amnesia and consolidation of memory. *Hippocampus*, *6*(6), 675–684.
Paller, K. A., & Wagner, A. D. (2002). Observing the transformation of experience into memory. *Trends in Cognitive Sciences*, *6*(2), 93–102.
Poser, B. A., Versluis, M. J., Hoogduin, J. M., & Norris, D. G. (2006). BOLD contrast sensitivity enhancement and artifact reduction with multiecho EPI: Parallel-acquired inhomogeneity-desensitized fMRI. *Magnetic Resonance in Medicine*, *55*(6), 1227–1235.
Scoville, W. B., & Milner, B. (1957). Loss of recent memory after bilateral hippocampal lesions. *Journal of Neurology, Neurosurgury and Psychiatry*, *20*(1), 11–21.
Sharon, T., Moscovitch, M., & Gilboa, A. (2011). Rapid neocortical acquisition of long-term arbitrary associations independent of the hippocampus. *Proceedings of the National Academy of Sciences of the USA*, *108*(3), 1146–1151.
Squire, L. R., & Alvarez, P. (1995). Retrograde amnesia and memory consolidation: a neurobiological perspective. *Current Opinion in Neurobiology*, *5*(2), 169–177.
Staresina, B. P., Duncan, K. D., & Davachi, L. (2011). Perirhinal and parahippocampal cortices differentially contribute to later recollection of object- and scene-related event details. *Journal of Neuroscience*, *31*(24), 8739–8747.
Staresina, B. P., Grey, J. C., & Davachi, L. (2009). Event congruency enhances episodic memory encoding through semantic elaboration and relational binding. *Cerebral Cortex*, *19*(5), 1198–1207.
Sugiura, M., Shah, N. J., Zilles, K., & Fink, G. R. (2005). Cortical representations of personally familiar objects and places: Functional organization of the human posterior cingulate cortex. *Journal of Cognitive Neuroscience*, *17*(2), 183–198.
Tendolkar, I., Arnold, J., Petersson, K. M., Weis, S., Anke, B.-D., van Eijndhoven, P., et al. (2007). Probing the neural correlates of associative memory formation: A parametrically analysed event-related functional MRI study. *Brain Research*, *1142*, 159–168.
Tse, D., Langston, R. F., Kakeyama, M., Bethus, I., Spooner, P. A., Wood, E. R., et al. (2007). Schemas and memory consolidation. *Science*, *316*(5821), 76–82.
Tse, D., Takeuchi, T., Kakeyama, M., Kajii, Y., Okuno, H., Tohyama, C., et al. (2011). Schema-dependent gene activation and memory encoding in neocortex. *Science*, *333*(6044), 891–895.
Tulving, E., & Kroll, N. (1995). Novelty assessment in the brain and long-term-memory encoding. *Psychonomic Bulletin and Review*, *2*(3), 387–390.
Tzourio-Mazoyer, N., Landeau, B., Papathanassiou, D., Crivello, F., Etard, O., Delcroix, N., et al. (2002). Automated anatomical labeling of activations in SPM using a macroscopic anatomical parcellation of the MNI MRI single-subject brain. *Neuroimage*, *15*(1), 273–289.
van Kesteren, M. T., Fernandez, G., Norris, D. G., & Hermans, E. J. (2010). Persistent schema-dependent hippocampal-neocortical connectivity during memory encoding and postencoding rest in humans. *Proceedings of the National Academy of Sciences of the United States of America*, *107*(16), 7550–7555.
van Kesteren, M. T., Rijpkema, M., Ruiter, D. J., & Fernandez, G. (2010). Retrieval of associative information congruent with prior knowledge is related to increased medial prefrontal activity and connectivity. *Journal of Neuroscience*, *30*(47), 15888–15894.
van Kesteren, M. T., Rijpkema, M., Ruiter, D. J., & Fernandez, G. (2011). *How a prior schema affects mnemonic processing*. Paper presented at the 5th International Conference on Memory, York, UK.
van Kesteren, M. T., Ruiter, D. J., Fernandez, G., & Henson, R. N. (2012). How schema and novelty augment memory formation. *Trends in Neurosciences*, *35*(4), 211–219.
Wagner, A. D., Shannon, B. J., Kahn, I., & Buckner, R. L. (2005). Parietal lobe contributions to episodic memory retrieval. *Trends in Cognitive Sciences*, *9*(9), 445–453.
Wang, S. H., & Morris, R. G. (2010). Hippocampal–neocortical interactions in memory formation, consolidation, and reconsolidation. *Annual Review of Psychology*, *61*(49–79), C41–44.
Watkins, M. J., & Gardiner, J. M. (1979). Appreciation of generate-recognise theory of recall. *Journal of Verbal Learning and Verbal Behavior*, *18*(6), 687–704.